HNPS Advances in Nuclear Physics

Vol 30 (2024)

HNPS2023

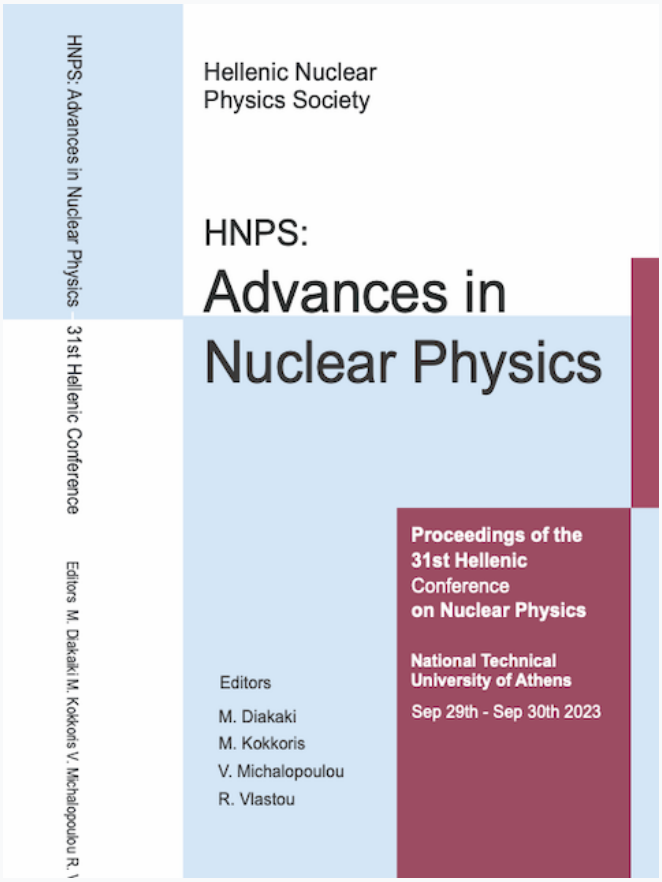

The energy dependence of the optical potential for weakly bound nuclei at sub- and near- barrier energies

Athena Pakou

doi: 10.12681/hnpsanp.6119

To cite this article:

Pakou, A. (2024). The energy dependence of the optical potential for weakly bound nuclei at sub- and near- barrier energies. *HNPS Advances in Nuclear Physics*, *30*, 1–10. https://doi.org/10.12681/hnpsanp.6119

The energy dependence of the optical potential for weakly bound nuclei at sub- and near-barrier energies

Athena Pakou*

Department of Physics and HINP, The University of Ioannina, Ioannina, Greece

Abstract We present a survey of our comprehensive studies for determining the energy dependence of the optical potential at sub- and near- barrier energies, for weakly bound nuclei. A new algorithm for describing the optical potential for ^{7}Be with mass and energy dependence on various targets is deduced and compared with existing optical potentials. The necessity of using global studies for determining the optical potential at sub- and near-barrier energies is outlined.

Keywords weakly bound nuclei, fusion, elastic scattering, optical potential, threshold anomaly

INTRODUCTION

Coupling channel effects for weakly bound nuclei appear strong at sub- and near- barrier energies due to their low breakup threshold for breakup or/and transfer reactions. The last twenty years the research in that direction by using either stable or radioactive projectiles was vivid and productive. Several review articles were written in that respect [1-5], and the reader can go through and discover information for specific systems. Some of the studies have to do with the stable but weakly bound lithium projectiles, ^{6,7}Li for their own sake, but also as predecessor studies with radioactive nuclei. Breakup and transfer effects or in general reaction mechanisms at below and near barrier energies manifest on the energy dependence of the optical potential producing variations in the standard threshold anomaly [6-7]. Differences occurred between ^{6}Li and ^{7}Li projectiles but also between light and heavy targets [8].

Our contribution to these issues has lasted for 20 years now and will be briefly outlined in the next sections. A new algorithm for describing the energy dependence of the optical potential will be presented together with the validation of it, via existing elastic scattering and fusion data at sub- and near-barrier energies.

PREVIOUS WORK

Our work for the energy dependence of the optical potential at sub- and near-barrier energies started twenty years ago with elastic scattering and α-production measurements of ^{6,7}Li on silicon targets. Measurements were performed at the 5.5 MV Tandem accelerator facility of the National Center of Scientific Research “Demokritos”. In Fig. 1, we present angular distributions for elastic scattering at below and near barrier energies. The analysis of these first pioneer results [9-11], and the reanalysis of existing data on heavier targets, underlined severe differences between the energy dependence of the optical potential for ^{6}Li and ^{7}Li (see Fig. 2). The optical model analysis was performed adopting a microscopic BDM3Y1 interaction [12] for the real part, double folded with the projectile and target densities. Assuming the same radial dependence as for the real part, this interaction was also used for the imaginary part, but with a different normalization factor. An inspection of Fig. 2 reveals that for ^{6}Li instead of the drop of the imaginary potential approaching the barrier from higher to lower energies, an

* Corresponding author: *apakou@uoi.gr*

increase occurs. Another interesting point is that for light targets either for ^{6}Li or ^{7}Li projectiles, a flat real potential is observed non-compatible with dispersion relations. Searching for the reasons behind these differences, we went through important measurements on various direct or compound channels [13-17], disentangling the various processes via particle – gamma coincidence experiments [13]. Our first results on reaction mechanisms are presented in Fig. 3, as the ratio of direct versus total reaction cross sections for ^{6}Li+^{28}Si. We should note that this system was comprehensively studied with measurements on elastic scattering [10], total reaction cross sections [17], breakup [16], transfer [14] and fusion [13,15].

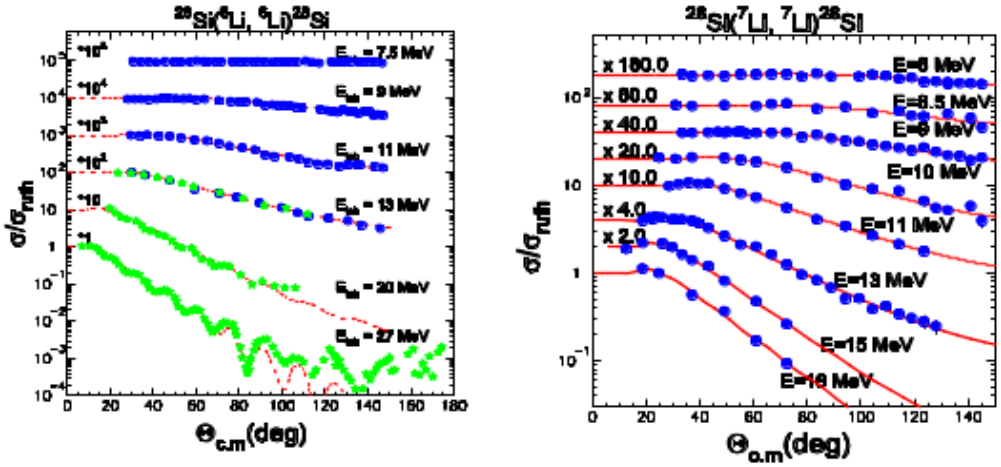

Figure 1. *Angular distributions of elastic scattering at sub- and near- barrier energies for ^{6}Li+^{28}Si (left) and ^{7}Li+^{28}Si (right). Figures are from Refs. [9-10].*

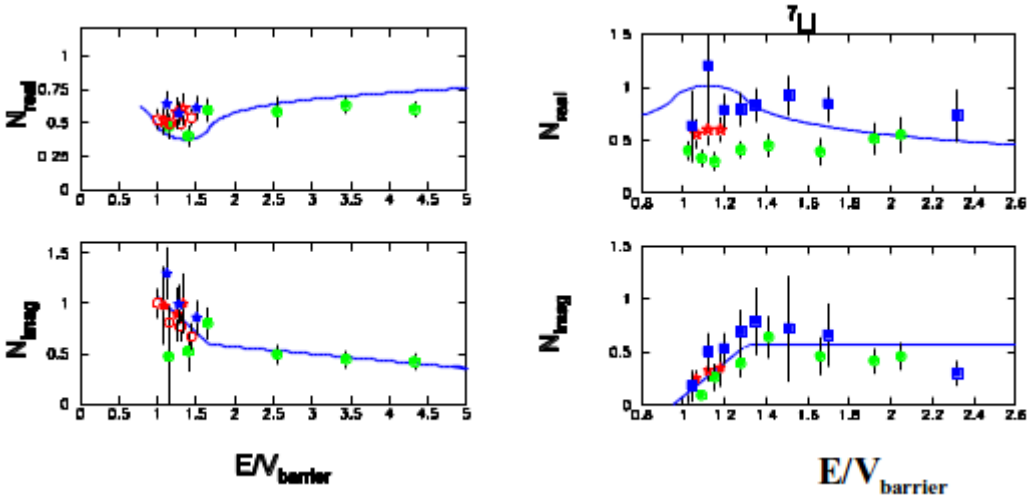

Figure 2. *The energy dependence of the optical potential extracted into a BDM3Y1 framework. (Left) for ^{6}Li and right for ^{7}Li. Data with green symbols are for a ^{28}Si target, with red color for ^{120}Sn and with blue color for ^{208}Pb. Figures are from Refs. [9-10].*

We can see from Fig. 3, that while at above barrier energies the compound mechanisms are strong, below barrier the direct ones become dominant. At the same figure (right) our predictions on light, medium, and heavy targets for weakly bound projectiles are presented with the red, green, and blue lines respectively. The predictions [18] were based on previous measurements on total reaction cross

sections and fusion cross sections, which were reduced accordingly, and ratios of direct (total-fusion) versus total reaction cross section were formed. These predictions are seen to be validated with data of ^{7}Be+^{28}Si [19], ^{8}B+^{58}Ni [20-21], ^{6}He+^{209}Bi [22] and ^{8}B+^{208}Pb [23], the last performed at deep sub-barrier energies, where breakup is dominant exhausting all the total reaction cross section.

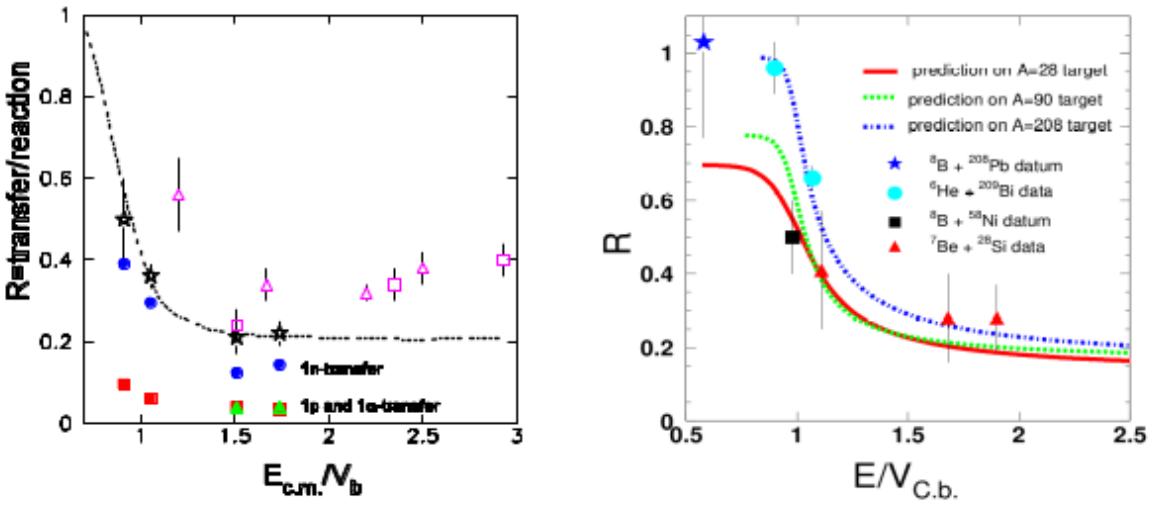

Figure 3. *The energy dependence of ratios direct to total reaction cross sections, (left) for ^{6}Li+^{28}Si are designated with the black stars. The decomposition of the direct part in 1n, 1p and 1α- transfer, is designated with the blue circles, red cubes and green triangles respectively. The Figure is from Refs. [13-14]. (right) Phenomenological predictions designated with a red line for a ^{28}Si target, with green line for ^{90}Zr and with a blue line for ^{208}Pb target. The data designated with the red triangles are for ^{7}Be+^{28}Si, the black box for ^{8}B+^{58}Ni, the ciel circles for ^{6}He+^{209}Bi and the blue star for ^{8}B+^{208}Pb. The Figure is from Ref. [23].*

While our research was on going for several years other studies became available with conflicting results. The questions that arose had to do with the real part of the optical potential which was different for the light and heavy targets, and the increasing behavior of the imaginary part for ^{6}Li against the decreasing one for ^{7}Li. It was soon understood that at sub- and near- barrier energies the elastic scattering is not sensitive to the nuclear potential since the Coulomb one becomes dominant. Therefore, other observables had to be determined complementary and considered for a more reliable extraction of the energy dependence of the optical potential. As such we had suggested the derivative of backscattering cross sections. The principle of this novel technique is described in detail in Refs. [24-26] and is summarized in Fig. 4, for ^{6,7}Li+^{28}Si. While this technique is a very sensitive complementary tool to elastic scattering for the determination of the optical potential, it can be rather applied to stable weakly bound projectiles where the beam flux is substantial, since the elastic scattering cross sections at backward angles is weak. Instead, someone can also rely on e.g. fusion and direct total cross section measurements.

This was understood when we started a program with radioactive beams and in fact with ^{7}Be. Elastic scattering and fusion measurements for ^{7}Be+^{28}Si were performed at the EXOTIC facility of the Laboratori Nazionali di Legnaro in Italy by our group, while we participated at the same Laboratory on elastic scattering measurements for the system ^{7}Be+^{208}Pb. Finally, we performed elastic scattering measurements for ^{7}Be+^{90}Zr at the Notre Dame *Trisol* radioactive facility-Indiana USA. All results were analyzed under the same phenomenological framework, by using the BDM3Y1 microscopic interaction, double folded with the projectile and target densities and appropriately normalized. The same

interaction but with different normalization factors was used for the imaginary part, assuming the same radial dependence with the real part.

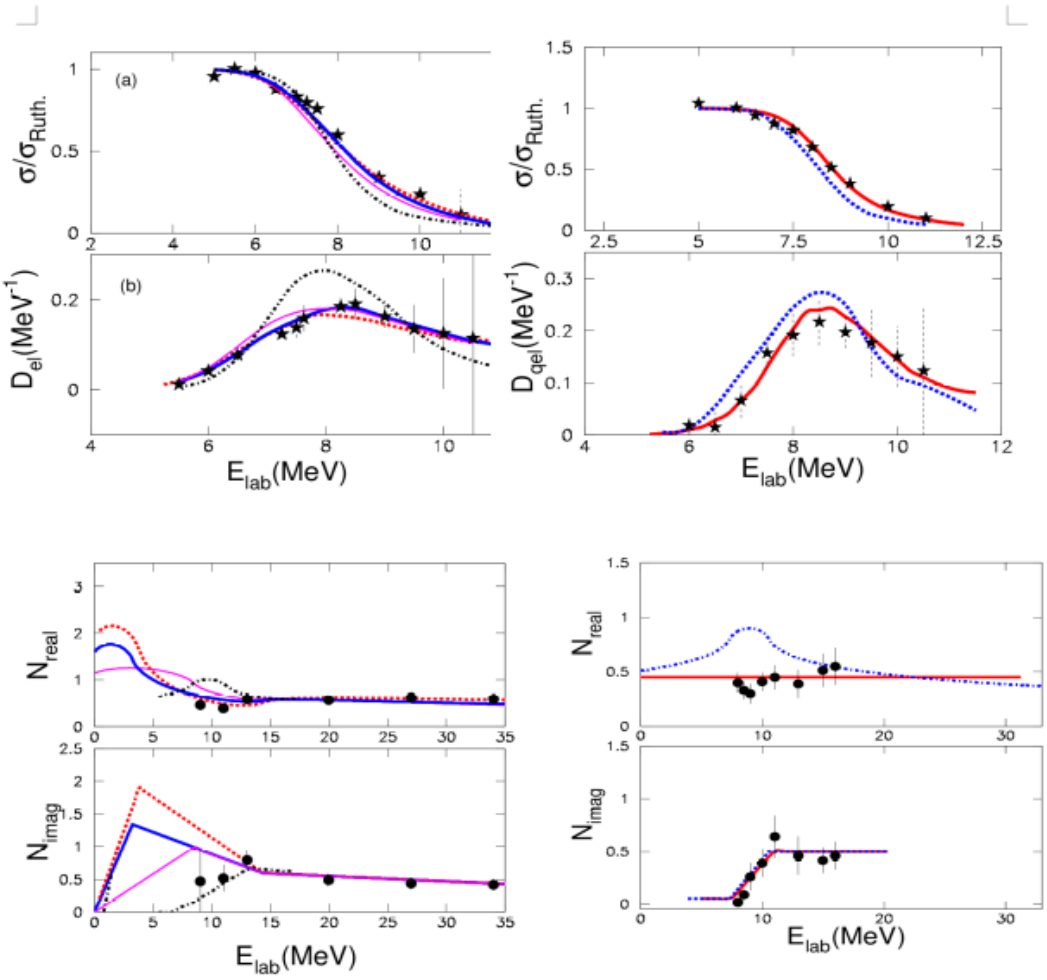

Figure 4. *Top: backscattering measurements; the excitation function of elastic backscattering cross sections at $\theta_{lab}=175^0$ and the corresponding derivatives (left) for $^6Li+^{28}Si$ and (right) for $^7Li+^{28}Si$. Bottom: Searching for the energy dependence of the optical potentials, considering the derivatives. Colors and type of lines are the same for excitation functions- derivatives and optical potentials The Figures are from Refs. [24-26].*

The energy dependence of the potential was extracted considering as a restriction existing fusion measurement for the same system or for nearby systems. The results for $^7Be+^{28}Si$, $^7Be+^{208}Pb$ and $^7Be+^{90}Zr$ are summarized in Figs. 5 and 6. It is seen that for heavy targets the energy dependence is the same as the one for ^7Li and therefore the same with the one exhibited by stable projectiles. For the lighter target, ^{28}Si, and for the real potential the reduction of the potential at higher energies persists at the lower ones, exhibiting a flat behavior not obeying the dispersion relations. Or it can be assumed that a strongly energy dependent breakup (transfer) polarization potential, on the presence of the anomaly been repulsive in nature, smooths out the real part. In other words, coupled channel effects are very weak and are not manifested either in elastic scattering with a potential anomaly or in fusion with an enhancement below barrier. For the heavier target the ^7Be results are like the ^7Li ones with the presence of the standard threshold anomaly, and the existence of a fusion enhancement below barrier. For the medium mass target, ^{90}Zr, we have a similar situation as for ^{208}Pb, but the existence of the anomaly

seems to be weaker (Fig.6). Also, for fusion a weaker enhancement of the cross sections below barrier exists.

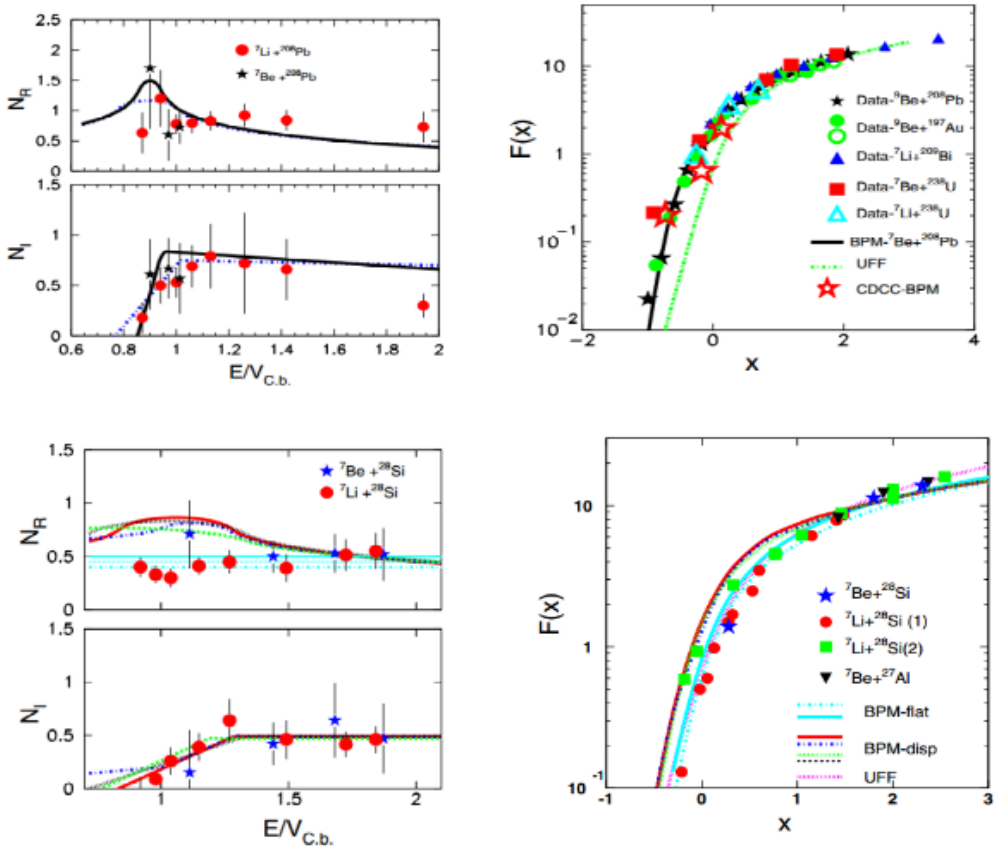

Figure 5. *Top: (left) The energy dependence of the optical potential for $^{7}Be+^{208}Pb$ and $^{7}Li+^{208}Pb$. Data are designated with the black stars and red circles respectively. The lines represent our dispersion analysis. (Right) reduced fusion data as appear in the figure insert are described very well with one barrier penetration calculations, adopting the potential at left with the black line. Bottom: The same but for ^{28}Si target The Figures are from Ref. [7]*

Considering as a guide all the above, we have proceeded in the determination of an algorithm for describing an optical potential for ^{7}Be projectiles. In this algorithm we considered the potential as energy and mass dependent below barrier and only mass dependent above barrier. Additionally for the above barrier energies, we consider two cases one for target mass numbers with A<90 and one for targets with A≥90.

THE OPTICAL POTENTIAL ALGORITHM

The potential was assumed of a Woods-Saxon form with a smooth mass dependent depth at above barrier energies, and an energy and mass dependent depth at below barrier energies. The reduced radii and diffusivities were fixed to the following values:

$$r_0^R = 0.815 r_0^I = 0.83$$

$$a^R = a^I = 0.855 \ fm\,,$$

with the radius R given as $R=r_0(A_1^{1/3}+A_2^{1/3})$ fm.

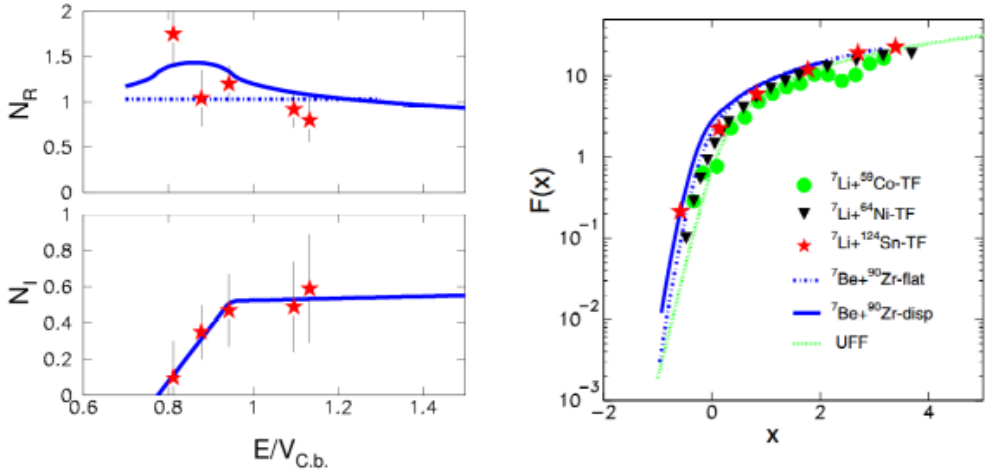

Figure 6. *(left)The energy dependence of the optical potential for $^{7}Be+^{nat}Zr$. (right) Reduced fusion functions for the systems indicated in the figure insert. Lines are one barrier penetration model calculations adopting the potentials indicated in the Figure left. The Figures are from Ref. [27].*

The depth of the real part of the potential at above barrier energies for targets with A=28 to 208, are parameterized as following:

$$V = 0.0006027 \times A^2 + 3.034 \times A - 11.69 \ \ MeV$$

At below barrier energies the same relation holds for targets with mass numbers $28 < A < 90$. At below barrier energies but for heavier targets the depth of the real potential is given as

$$\frac{V}{A} = 3.703 \times \frac{E}{V_B}^{-2.0865} \text{MeV}$$

For the imaginary part and for all targets the potential above the barrier can be written as

$$0.9666 \times A + 56.93 MeV$$

Below barrier an energy dependence has to be taken into account as

$$\frac{W}{A} = 9.45126 \times \left(\frac{E}{V_B}\right)^2 - 15.578 \times \left(\frac{E}{V_B}\right) MeV$$

Or as

$$\frac{W}{A} = \left(1.25 \times \frac{E}{V_B}^{\square} - 0.305\right) MeV \ \ for \frac{E}{V_B} > 0.865$$

And

$$\frac{W}{A} = 0.767 MeV \ ,$$

where A is the target mass number, E the beam energy at the center of mass and V_B the Coulomb barrier according to Broglia [28] given below as

$$V_B = \frac{R_f \times 1.44 \times Z_1 \times Z_2}{R_2} \ ,$$

with

$$R_f = 1 - \frac{0.63}{R_2}$$

And

$$R_2 = \left(1.07 \times \left(A_1^{\frac{1}{3}} + A_2^{\frac{1}{3}}\right) + 2.72\right) fm$$

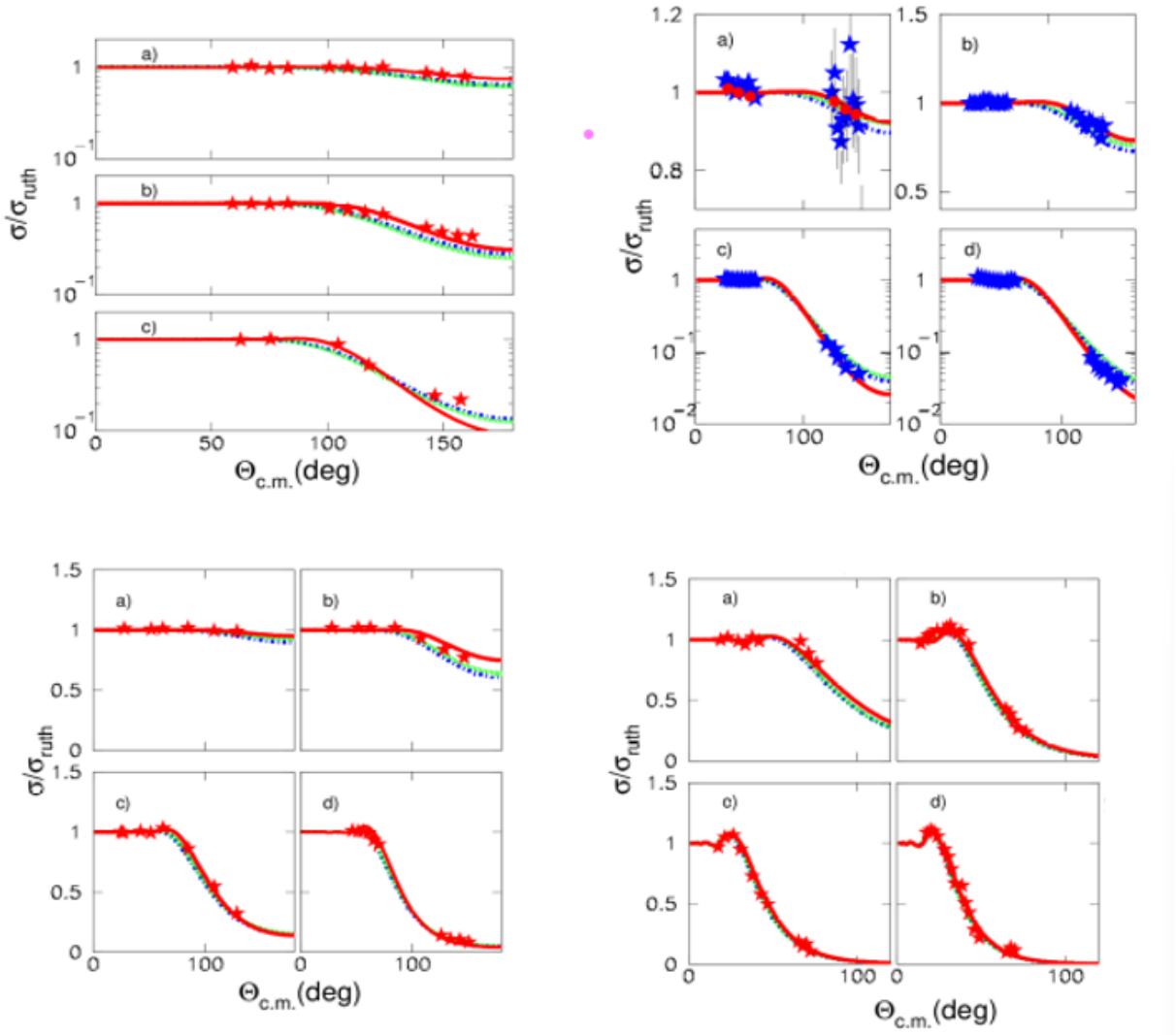

Figure 7. *(top-left Ref.[31)Elastic scattering data for $^{7}Be+^{208}Pb$ at a) 37.6 MeV, b) 40.5 MeV, c) 42 MeV, (top-right Ref. [27]) for $^{7}Be+^{90}Zr$ at a) 19.7 MeV, b) 21.3 MeV, c) 27.1 MeV, d) 27.5 MeV, (bottom-left Ref.[32]) for $^{7}Be+$ ^{58}Ni at a) 15.1 MeV, b) 17.1 MeV, c) 19.9 MeV, d) 21.5 MeV and (bottom-right Ref. [19]) for $^{7}Be+^{28}Si$ at a) 12.9 MeV, b) 16.7 MeV, c) 19.5 MeV, d) 21.7 MeV, are compared with calculations adopting the present potential – solid red line- and the Cook potential for $^{6,7}Li$, green and blue lines.*

Calculations with the above potential for elastic scattering at sub- and near- barrier energies are compared with data for $^{7}Be+^{208}Pb$, $^{7}Be+^{90}Zr$, $^{7}Be+^{58}Ni$ and $^{7}Be+^{28}Si$ in Fig. 7. The agreement with the data is excellent. The calculations were repeated with the Cook potential [29] as modified in ref. [30], extracted for ^{6}Li and ^{7}Li on various targets. The agreement with the data is good.

Subsequently, calculations were repeated with the present and Cook potentials for ^{7}Li on various targets and the results are summarized in Figure 8. The agreement between data and calculations with

the present potential is fair but with the Cook is very good. However, final conclusions can only be reached if we look the agreement with data of another observable like fusion. Indeed in Fig. 9-left-, we present one barrier penetration calculations with the present or the Cook potential for ^{6}Li and ^{7}Li for ^{7}Be+^{208}Pb. Obviously only the present potential can predict the enhancement below barrier while the Cook remains either consistent with a Wong prediction or even below it. This is also evident from the same figure (right), where we compare fusion calculations with the present potential and the Cook ones in comparison with the Wong prediction. More details about our algorithm can be found in Ref. [36].

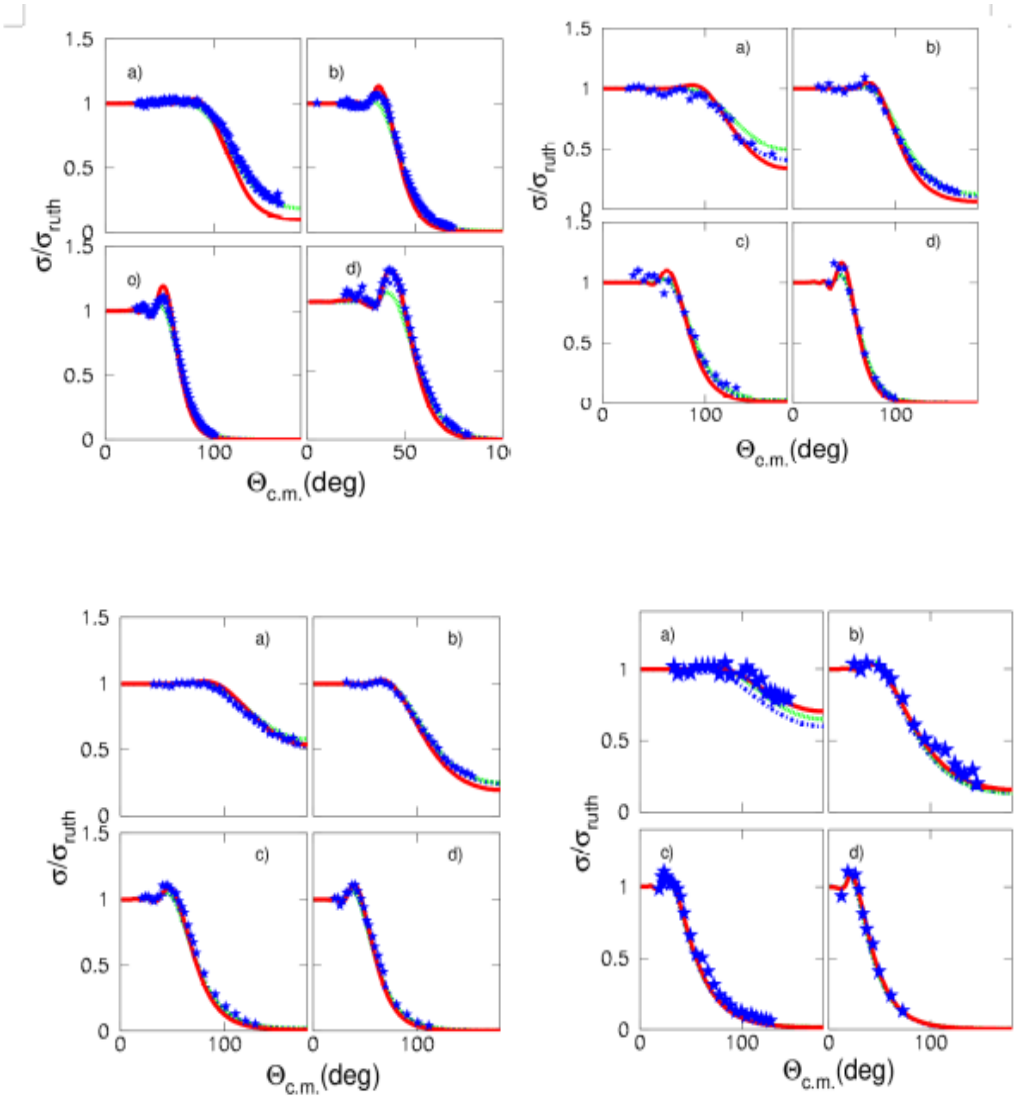

Figure 8. *Elastic scattering data (top-left-from Ref. [33]) for ^{7}Li+^{208}Pb, (top-right Ref. [34]) for ^{7}Li+^{138}Ba, (bottom-left ref. [35]) for ^{7}Li+^{64}Zn and (bottom-right Ref. [9]) for ^{7}Li+^{28}Si, are compared with calculations adopting the present potential-solid red line- and the Cook potential for ^{6,7}Li-green and blue lines.*

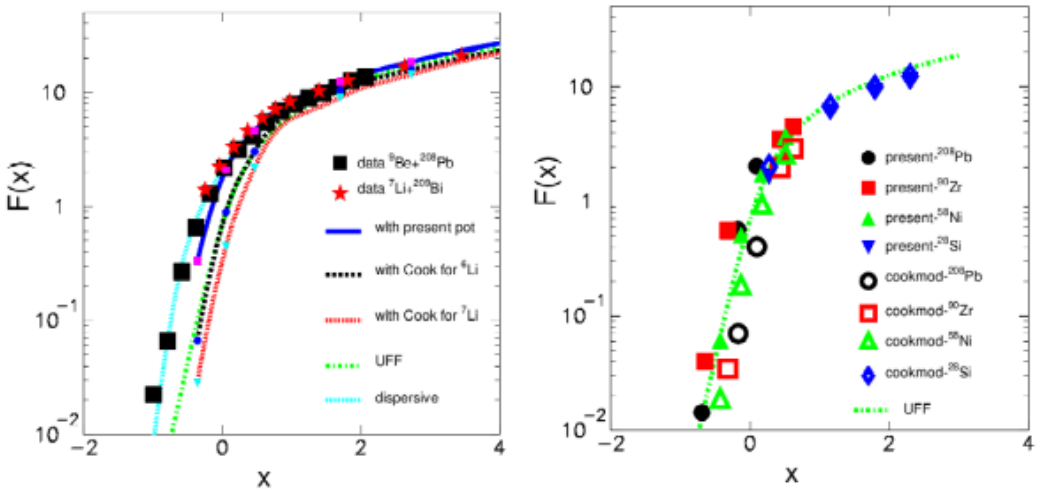

Figure 9. *(left) Reduced fusion cross sections for data as appear in the insert, are compared with our one barrier penetration calculations for ^{7}Be+^{208}Pb, adopting the present as well as the Cook potentials. (right)one barrier calculations for ^{7}Be+^{208}Pb, ^{7}Be+^{90}Zr, ^{7}Be+^{58}Ni and ^{7}Be+^{28}Si adopting the present potential and the Cook ones are compared amongst themselves as well as with the Wong predictions. See explanations in the insert.*

Summary

The last twenty years we have performed research on elastic scattering and reaction channels with weakly bound projectiles at sub- and near-barrier energies. Among other issues, the outcome of this research had to do with the determination of the optical potential and the relevant reaction mechanisms. It was found that:

- The energy dependence of the optical potential at sub- and near-barrier energies is different for ^{6}Li and ^{7}Li
- The energy dependence of the potential for ^{7}Be resembles that of its mirror ^{7}Li
- The energy dependence of the optical potential for ^{7}Be and therefore ^{7}Li is different for light than for heavy targets. For light targets the reduction of the potential persists till very low energies, exhibiting a flat behavior. This may imply the absence of the anomaly with the absence of causality or the presence of the anomaly with a polarization potential strongly dependent on energy and smoothing out the anomaly. The consequence of a flat real potential is consistent with no fusion enhancement below barrier. For heavier targets the standard anomaly is observed, and an enhancement of fusion occurs.
- For a reliable extraction of the optical potential at sub- and near-barrier energies, complementary observables to elastic scattering are necessary. In this direction fusion can play a critical role.
- An algorithm for the description of the optical potential for ^{7}Be is suggested, validated both by elastic scattering and fusion cross sections.

Acknowledgments

We warmly acknowledge the invaluable contribution in this research of Nicola Alamanos and his former group at Saclay, also of Anastasios Lagoyannis from NCSR Demokritos and of Michael Kokkoris from NTUA. The last ten years the contribution of Akis Sgouros and Vassilis Soukeras today at INFN and University of Catania, was critical and invaluable. Finally, we warmly acknowledge the contribution of the accelerator staffs at NCSR Demokritos-Greece, LNL-Italy and the post-graduate students of Notre Dame-Indiana-USA for running the accelerator and our colleagues Marco Mazzocco and Patrick O'Malley, for producing the radioactive beams at the EXOTIC facility of LNL and the *Trisol* facility at Notre Dame, but not only.

References

[1] L.F. Canto et al., Phys. Rep. 424, 1 (2006)
[2] N. Keeley et al., Prog. Part. Nucl. Phys. 59, 579 (2007)
[3] N. Keeley et al., Prog. Part. Nucl. Phys. 63, 396 (2009)
[4] P.R.S. Gomes et al., J. Phys. G: Nucl. Part. Phys. 31, S1669 (2005)
[5] A. Pakou et al., Eur. Phys. J. A 58, 8 (2022)
[6] G.R. Satchler, Phys. Rep. 199, 147 (1991)
[7] C. Mahaux, H. Ngo, G.R. Satchler, Nucl. Phys. A 449, 354 (1986)
[8] O. Sgouros et al., Phys. Rev. C 106, 044612 (2022)
[9] A. Pakou et al., Phys. Rev. C 69, 054602 (2004)
[10] A. Pakou et al., Phys. Lett. B 556, 21 (2003)
[11] A. Pakou et al., Phys. Rev. Lett. 90, 202701 (2003)
[12] D.T. Khoa et al., Phys. Lett. B 342, 6 (1995)
[13] A. Pakou et al., internal report (2007), http://npl.physics.uoi.gr/preprints.htm
[14] A. Pakou et al., Phys. Rev. C 76, 054601 (2007)
[15] A. Pakou et al., Eur. Phys. J. A 39,187 (2009)
[16] A. Pakou et al., Phys. Lett. B 633, 691 (2006)
[17] A. Pakou et al., Nucl. Phys. A 784, 13 (2007)
[18] A. Pakou et al., Eur. Phys. J. A 51, 55 (2015)
[19] O. Sgouros, Phys. Rev. C 95, 054609 (2017)
[20] V. Guimaraes et al., Phys. Rev. Lett. 84, 1862 (2000)
[21] J.J. Kolata et al., Phys. Rev. C 63, 024616 (2001)
[22] E.F. Aguilera et al., Phys. Rev. Lett. 84, 5058 (2000)
[23] A. Pakou et al., Phys. Rev. C 102, 031601(R) (2022)
[24] K. Zerva et al., Phys. Rev. C 80, 017601 (2009)
[25] K. Zerva et al., Phys. Rev. C 82, 044607 (2010)
[26] K. Zerva et al., Eur. Phys. J. A 48, 102 (2012)
[27] K. Palli et al., Phys. Rev. C 107, 064613 (2023)
[28] R.A. Broglia and A. Winther, Heavy Ion Reactions, Vol. I: Elastic and Inelastic Reactions (The Benjamin/Cummings Publishing Company, Inc, San Francisco, 1981)
[29] J. Cook, Nucl. Phys. A 388, 153 (1982)
[30] V.A.B. Zagatto et al., Phys. Rev. C 107, 044604 (2023)
[31] M. Mazzocco et al., Phys. Rev. C 100, 024602 (2019)
[32] M. Mazzocco et al., Phys. Rev. C 92, 024615 (2015)
[33] N. Keeley et al., Nucl. Phys. A 571, 326 (1994)
[34] A.M.M. Maciel et al., Phys. Rev. C 59, 2103 (1998)
[35] J.P. Fernandez-Garcia et al., Phys. Rev. C 92, 054602 (2015)
[36] A. Pakou, Phys. Rev. C 109, 014609 (2024)